Volume 1 | Number 1 | Jan 2013 | Pages 1–100

Polymer Chemistry

www.rsc.org/polymers

ROYAL SOCIETY OF CHEMISTRY

ROYAL SOCIETY OF CHEMISTRY

www.rsc.org/polymers

Journal Name

Polymer Chemistry

ARTICLE TYPE

Polymerization and Degradation of Aliphatic Polyesters Synthesized by Atom Transfer Radical Polyaddition

Yu-Min Han,[a] Hsin-Hua Chen,[a] and Chih-Feng Huang[a],*

Two AB*-type inimers (4-vinylbenzyl 2-bromo-2-isobutryrate (VBBiB) and 4-vinylbenzyl 2-bromo-2-phenylacetate (VBBPA)) were synthesized and used to obtain aliphatic polyesters through atom transfer radical polyaddition (ATRPA). First, we optimized the ATRPA of VBBiB at a moderate temperature (<25 °C) using a commercially available $CuBr_2/Cu(0)/dNBpy$ system; however, reaction run at 70 °C exhibited self-degrading behavior, as revealed by molecular weight (MW) variations in GPC traces and evidence for a five-
10 membered-ring lactone structure (5-(4-(bromomethyl)phenyl)dihydro-3,3-dimethylfuran-2(3H)-one) in ^1H NMR spectra. We suspected that the structural rearrangement occurred through ring-closure depolymerization of PVBBiB induced by the pendant bromine atoms serving as leaving groups. Accordingly, by varying the leaving group affinities, we performed a series of model reactions that guided us toward polymers with stable backbones. We thus synthesized three additional aliphatic polyesters PVBCiB (C: chloro), PVBBPA, and PVBAiB (A: azido) through ATRPA of VBBiB with halogen exchange, ATRPA of VBBPA, and azido substitution of bromine atoms,
15 respectively. For PVBCiB and PVBBPA, we confirmed the structures of these aliphatic polyesters, which we obtained with high MWs (e.g., $M_{w,PVBBPA}$ = 25,550), fulfilling our desire to obtain high-MW aliphatic polyesters through the embryonic ATRPA method. From comparisons of the four aliphatic polyesters, PVBBiB and PVBCiB displayed significant self-degrading profiles over periods of several days, whereas PVBBPA and PVBAiB did not. This study unveils the limitations (relating to lactonization) of ATRPA involving AB*-type inimers, and also widens the scope of the process.

Introduction

20 In recent decades, aliphatic polyesters (e.g., polylactides, poly(ε-caprolactone)s, polyglycolides, and related copolymers) have become important materials because of their (bio)degradability and biocompatibility. Cleavable linkages (e.g.,
25 ester, amide, polysulfide) are produced or introduced into the backbones of these aliphatic polyesters during their polymerization. The methods used most widely for the production of aliphatic polyesters,[1-5] nevertheless, are not compatible with many functionalities, making it difficult to
30 present diverse functional groups on the polymer backbones. Thus, several novel synthetic approaches, inspired by efficient organic reactions for producing functional aliphatic polyesters, have been adapted. For example, linear poly(amino ester)s and poly(thio ester)s with functional groups have been prepared
35 through Michael-type polyadditions of diacrylates with diamines and dithiols, respectively.[6-9] Copolymerization of epoxides and cyclic anhydrides has been a facile and simple method for preparing functionalized polyesters.[10-12] Efficient approaches have been demonstrated toward functionalized polyester-based
40 copolymers through Passerini reactions and through acyclic diene metathesis (AMDET)[13-15] or Baylis–Hillman reactions.[16, 17]

Conventional free radical (co)polymerizations, which are commonly applied industrially, can also be used to synthesize degradable polymers.[18] With the developments of reversible
45 deactivation radical polymerizations (RDRPs), the incorporation of cleavable group can be accomplished relatively effortlessly through the use of cleavable initiators or monomers. Radical ring-opening polymerizations (RROPs) of several cyclic monomers have been conducted as a fascinating approach toward aliphatic
50 polyesters with a variety of bio- and chemodegradable linkages introduced into their backbones.[19-22] Although RROP is an analogue of RDRP, the RROP method faces several challenges that limit its applicability at present to a narrow range of functionalized monomers. Among established RDRP techniques,
55 atom transfer radical polymerization (ATRP),[23-26] extended from atom transfer radical addition (ATRA),[27] is one of the most widely used controlled radical polymerization methods because it can be applied to a wide range of functionalized monomers. Thanks to detailed mechanistic studies, a vast family of atom
60 transfer radical reactions can be gathered, including ATRP[28] and its variants,[29] ATRA,[30] Cu(0)-mediated controlled radical polymerization,[31-33] atom transfer radical coupling (ATRC),[34] atom transfer nitroxide radical cross coupling (ATNRC),[35] atom transfer self-condensing vinyl polymerization (ATSCVP),[36-38]
65 atom transfer radical polyaddition (ATRPA),[39, 40] and simultaneous chain- and step-growth radical polymerization.[41, 42] These methods facilitate highly efficient "divergent" and "convergent" approaches for the synthesis of unique macromolecules, in terms of their composition, topology, and
70 functionality.

Recently, novel analogues of aliphatic polyesters with functional groups on their polymer backbones can be obtained through manipulation on the different activation/deactivation rate

Polymer Chemistry Accepted Manuscript

constants of the initiator structures when using ATRPA. Literatures have demonstrated the related aliphatic polyesters for the applications of degradable antibacterial polymers[43] and degradable thermoresponsive polyesters.[44] The preliminary discussion of the preparation of aliphatic polyesters through ATRP of AB*-type inimers was reported by Matyjaszewski et al.[38] The first idea of utilizing metal-catalyzed radical polyaddition in a precise manner was demonstrated by Kamigaito et al., who synthesized aliphatic polyesters containing a large number of functionalizable chlorine atoms along the polyester backbone.[39, 45,] To reach high conversion (>90%), however, the reaction time on the order of tens of days were necessary, due to the intrinsically low addition reactivity of the formed radical to the vinyl bond. Li et al., who identified the term "atom transfer radical polyaddition," were the first to perform elegant approaches by using an AB* inimer and AA/B*B* monomer pairs containing methacrylate-type initiating sites and styrene units.[37] After the atom transfer reactions had occurred, two kinds of initiating sites were generated: one similar to a less-active 1-(bromoethyl)benzene (PEBr) and the other similar to a highly active ethyl α-bromoisobutyrate (EBiB). Because of the significant difference in activation rate constants between these two initiating sites ($k_{a,EBiB}/k_{a,PEBr}$ = $ca.$ 16 at 35 °C),[28] the less-active PEBr site could be "frozen" while rapid "polyaddition" occurred between the more-active EBiB site and the vinyl bond under specific conditions (i.e., CuBr$_2$/Cu(0)/BPMOA complex at 0 °C). This effective pair—a methacrylate-type initiating site and a styrene unit—not only shortened the reaction time but also allowed aliphatic polyesters to be obtained with functionalities along their backbones. Restricted to the current scope of ATRPA, the newly formed alkyl halide generated through ATRPA should be unreactive/inactive toward the metal complex, with a low-temperature reaction conceivable to achieve a perfect monoadduct by turns.

Thus, we expected that variations of the competitive reaction factors—inimer structure, catalyst system, and reaction temperature—might provide an inexpensive and straightforward route to obtain functional degradable aliphatic polyesters. As shown in Scheme 1, four types of aliphatic polyester (poly(4-vinylbenzyl 2-bromo-2-isobutyrate) (PVBBiB), poly(4-vinylbenzyl 2-chloro-2-isobutyrate) (PVBCiB), poly(4-vinylbenzyl 2-bromo-2-phenylacetate) (PVBBPA), and poly(4-vinylbenzyl 2-azido-2-isobutyrate) (PVBAiB)) were targeted and their related AB* inimers and precursors were synthesized. Through ATRPA with common copper complex, we demonstrated that aliphatic polyesters possessing degradable linkages in backbone can be also obtained. We further studied the detailed conditions of ATRPA and investigated the degradation behavior of these polymers to optimize and evaluate this new category of synthesizable aliphatic polyesters.
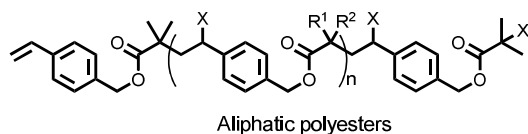
Scheme 1. Synthesis of aliphatic polyesters (PVBBiB: $R^1 = R^2 = CH_3$, X = Br; PVBCiB: $R^1 = R^2 = CH_3$, X = Cl; PVBBPA: $R^1 = H$, R^2 = phenyl, X = Br; PVBAiB: $R^1 = R^2 = CH_3$, X = N$_3$).

Experimental

Materials. 4-Vinylbenzyl chloride (VBC, 90%), 2-bromoisobutyryl bromide (BiB, 97%), 4,4-dimethylaminopyridine (DMAP, 99%), N,N'-dicyclohexylcarbodiimide (DCC, 99%), triethylamine (TEA, 99.5%), α-bromophenylacetic acid (BPA, 98%), copper(II) bromide (CuBr$_2$, 99%), copper(II) chloride (CuCl$_2$, 99%), 4,4′-dinonyl-2,2′-bipyridine (dNBpy, 97%), alumina (neutral), and Dowex® 50WX8 (H form/200-400 mesh) were purchased from Sigma–Aldrich. Sodium acetate (98%), 1-methyl-4-vinylbenzene (MVB, 98%), copper wire (d = 0.5 mm), copper powder (150 mesh, 99.5%), sodium trinitride (NaN$_3$, 98%), benzyl alcohol (BzOH, 99%), tetrabutyl ammonium chloride (TBAC, 95%), copper(I) chloride (CuCl, 97%), and 2,2′-bipyridine (Bpy, 99%) were purchased from Alfa. CuCl was washed with acetic acid to remove soluble oxidized species, filtered, washed with absolute ethanol and dried in vacuum. 4-Vinylbenzyl alcohol (VBA), 4-vinylbenzyl 2-bromo-2-isobutyrate (VBBiB), 4-vinylbenzyl 2-bromo-2-phenylacetate (VBBPA), 4-methylbenzyl 4-bromo-2,2-dimethyl-4-p-tolylbutanoate (BzBDT), 4-methylbenzyl 4-chloro-2,2-dimethyl-4-p-tolylbutanoate (BzCDT), and PVBAiB were synthesized according to literature precedents (see Supporting Information: Figs. S1–S4).[46, 47] All solvents were purified through distillation prior to use.

Synthesis of PVBBiB/PVBBPA through ATRPA. A typical example for ATRPA of VBBiB: Anisole (1 mL), VBBiB (1.13 mL, 4.00 mmol), CuBr$_2$ (18 mg, 0.08 mmol), and dNBpy (196 mg, 0.48 mmol) were added to a Schlenk flask and degassed with three freeze/pump/thaw cycles. The flask was backfilled with N$_2$ and copper wire (L = 5.8 mm; d = 0.5 mm) was added to the frozen solution. The flask was sealed and deoxygenated through two additional freeze/pump/thaw cycles (VBBiB/CuBr$_2$/Cu(0)/dNBpy = 50/1/2/6; [VBBiB]$_0$ = 1.8 M). An initial sample was taken and the solution was stirred at a desired temperature for a period of time. Samples were withdrawn periodically via syringe to measure the inimer conversion (by gas chromatography (GC)) and molecular weight (MW) of the polymer (by gel permeation chromatography (GPC)). The polymerization was stopped by cooling the flask in an ice bath, exposing the content to air, and diluting the mixture with THF. The fresh mixture was then passed through an alumina column and precipitated into cold petroleum ether. The resulting white powder was filtered, dried overnight under vacuum, and stored in a fridge (yield: 35%).

Halogen exchange for the syntheses of PVBCiB and BzCDT. Using atom transfer–induced halogen exchange method, a aliphatic polyester and a model compound featuring chlorine leaving atom were targeted. For the preparation of PVCBiB, the reagents and ATRPA steps were same as those described above, except for the use of CuCl$_2$ (i.e., VBBiB/CuCl$_2$/Cu(0)/dNBpy = 50/1/0.04/0.12; [VBBiB]$_0$ = 1.8 M; yield: 40%). For the preparation of BzCDT, the precursor benzyl 2-chloro-2-methylpropanoate (BzCMP) (see Supporting Information) was synthesized from benzyl 2-bromo-2-methylpropanoate (BzBMP), CuCl, CuCl$_2$, and Bpy in acetone at 50 °C for 2 days (BzBMP/CuCl/CuCl$_2$/Bpy = 1/2/1/6; [BzBMP]$_0$ = 0.1 M; yield: 68%). ATRA was conducted with BzCMP, MVB, CuCl$_2$, copper powder, and dNBpy in THF at 25 °C

(BzCMP/MVB/CuCl$_2$/Cu(0)/dNBpy = 25/25/1/2/6; [BzCMP]$_0$ = 0.3 M). The crude product was purified using Dowex® 50WX8 to remove metal complexes and then passed through a silica column (EtOAc/hexane, 1:10 (v/v)) to obtain BzCDT (yield: 22%).

Synthesis of VBBPA. A 500-mL two-neck round-bottomed flask was dried and refilled with N$_2$. VBA (9.4 g, 70 mmol), α-bromophenylacetic acid (15 g, 70 mmol), and dry CH$_2$Cl$_2$ (200 mL) were charged into the flask. A mixture of DMAP (0.85 g, 2.0 mmol), DCC (14.4 g, 70.0 mmol), and dry CH$_2$Cl$_2$ (50 mL) was added dropwise to the flask with stirring at 0 °C for a few hours. The temperature of the mixture was elevated to 40 °C, where it was maintained for an additional 24 h under N$_2$. The solids were filtered off; the filtrate washed with 1 M HCl$_{(aq)}$, 1 M NaOH$_{(aq)}$, and water and then dried (MgSO$_4$). After evaporation of the solvents, the residue was purified through a silica column (EtOAc/hexane, 1:10 (v/v)) to give a yellowish liquid (yield: 74%); ^{1}H NMR (400 MHz, CDCl$_3$, δ = ppm): 5.20 (dd, PhCH_2, 2H), 5.28, 5.75 (d, CH_2=CH, 2H), 5.40 (s, PhCH(C=O)Br, 1H), 6.68–6.75 (dd, CH$_2$=CH, 1H), 7.27–7.40 and 7.51 (m, C$_6$$H_4$ and C$_6$$H_5$, 9H). ^{1}H NMR and FT-IR spectra are presented in Figure S5.

Examinations of self-degradation behaviors. The obtained polymers PVBBiB, PVBCiB, PVBBPA, and PVBAiB were charged individually into several vials and capped. Over a period of several days under ambient conditions (20±5 °C and RH = 75± 5%), the samples were monitored using GPC with a constant concentration of 4 mg/mL. The normalized decomposition and byproduct ratios were defined in terms of the intensity at time t with respect to the initial intensity (i.e., I_t/I_{t0}) of the main GPC traces. The degraded resultants and the model reactions were further analyzed using ^{1}H NMR spectroscopy.

Characterization. ^{1}H NMR spectra of samples in CDCl$_3$ were recorded using a Varian Inova 400 NMR spectrometer; the chemical shifts were calibrated by setting the chemical shift of residual CHCl$_3$ at 7.26 ppm. FT-IR spectra were recorded using a Nicolet Avatar 320 FT-IR spectrometer; 32 scans were collected at a resolution of 1 cm^{-1}. The liquid samples were cast onto a KBr disk and dried under vacuum. The sample chamber was purged with N$_2$ to maintain film dryness. Conversions of inimers were monitored using a Hewlett Packard 5890 series II gas chromatograph equipped with an FID detector and a CNW CD-5 column (30 m), with anisole as the internal standard. GPC was conducted at 40 °C in tetrahydrofuran (THF; flow rate: 1 mL/min) using an apparatus equipped with a Waters 515 pump, a Waters 410 differential refractometer, a Waters 486 absorbance detector, and two PSS SDV columns (Linear S and 100 Å pore size) to obtain values of M_n, M_w, and $Đ$ (i.e., M_w/M_n). Monodisperse polystyrene standards were used for calibration.

Results and discussion

1. Influence of temperature on the side reactions during ATRPA of VBBiB.

In our first attempt, we evaluated and optimized the ATRPA of VBBiB using a commercially available copper complex (CuBr$_2$/Cu(0)/dNBpy) at various reaction temperatures. Figure 1A presents profiles of the conversion with respect to the reaction

time; here, the reaction rate was faster at elevated temperatures. For the reaction performed at 0 °C (curve d in Figure 1A), over 7 days were required to reach a conversion of 80%, implying that CuBr$_2$/Cu(0)/dNBpy was less efficient as a catalyst as those reported previously.[28] In contrast, we obtained high conversions (>90%) within less than 70 h for the reactions run at 25 and 10 °C (curves b and c, respectively, in Figure 1A) and even within only approximately 20 h for the reaction run at 70 °C (curve a in Figure 1A). Figure 1B displays plots of M_n/$Đ$ vs conversion. Curves a–c reveal significant increases of M_n and $Đ$ in the stage of the higher conversions, suggesting that the reaction followed a step–growth mechanism. Notably, only low M_n (ca. 400 at 94% conv.) appeared in curve d, implying side reactions occurred at high temperature. The side reactions during the ATRPA of the VBBiB inimer between the bromoisobutyrate moiety and the vinyl bond presumably resulted from several possible scenarios: (1) higher temperature resulted in faster generation of methacrylic radical and accompanied more terminations of radical disproportionation/coupling; (2) higher temperature resulted in more branched linkages through self-condensing vinyl polymerization; and (3) intramolecular addition of an ω-carbon radical to an α-vinyl bond (Scheme 2). Thus, although a higher temperature accelerated the reaction rate, it also led to some undesired reactions.
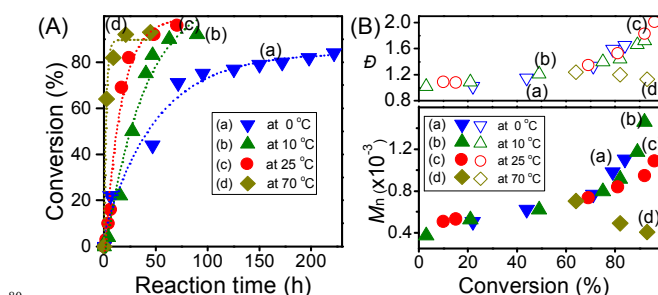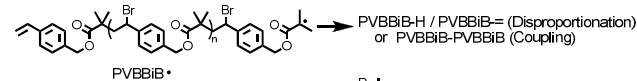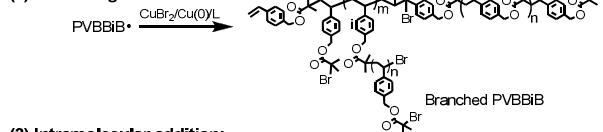

Figure 1. Kinetic plots of ATRPA with different temperature: (A) conversion vs time and (B) M_n/$Đ$ vs conversion (VBBiB/CuBr$_2$/Cu(0)/dNBpy = 50/1/2/6 in anisole; [VBBiB]$_0$ = 1.8 M).
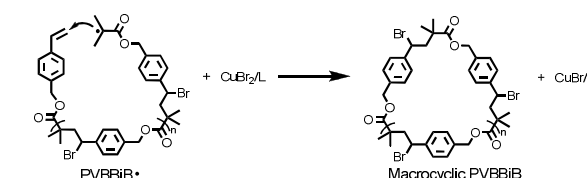

Scheme 2. Side reactions during the ATRPA of VBBiB: (1) termination of methacrylic radical, (2) chain branching from a less-active initiating site, and (3) intramolecular ω-carbon

radical–α-vinyl addition.

We recorded ^{1}H NMR spectra (Figure 2) to understand the detailed microstructures of the products. For the reactions run at 25, 10, and 0 °C (Figures 2b–2d, respectively), signals appeared for the aliphatic polyester of PVBBiB. Figure 2c provides detailed peak assignments. For the reaction run at 70 °C (Figure 2a), signals for the aliphatic polyester of PVBBiB were absent; instead, we observed significant signals presumably caused by side reactions. Signals arising from radical disproportionation/coupling and chain branching were not obvious, but other strong signals were present, implying that side reactions other than those proposed in Scheme 2 were significant for the reaction run at 70 °C. The spectra of Figures 2a and 2b feature similarly minor peaks. Hence, a higher temperature enhanced the side reactions. Entries 1–5 in Table 1 summarize the reaction conditions and characterization data. We inferred that the side reaction resulted from self-degradation of the linkages of the backbone during polymerization.
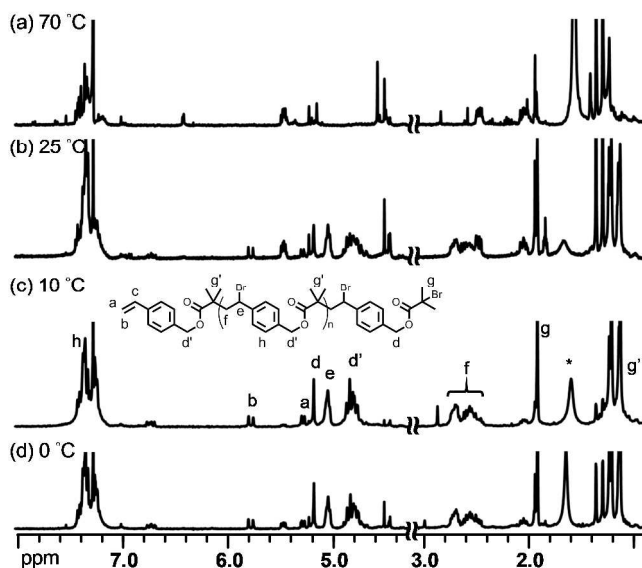

Figure 2. ^{1}H NMR spectra (400 MHz, CDCl$_3$) of the ATRPA resultants in Figure 1.

Table 1. Conditions for ATRPA of VBBiB, with characterization data of the products.

Entry[a]	Compositions[a]	Temp. (°C)	Time (h)	Conv. (%)	$M_w{}^b$	Đ[b]
1	50/6/1	0	222	84	1690	1.24
2	50/6/1	10	72	90	2660	1.54
3	100/6/1	10	168	97	2240	1.45
4	50/6/1	25	70.5	90	2800	1.37
5	50/6/1	70	45	93	528	1.59
6	50/6/1/2	10	63	94	4400	1.78
7	50/10/4/1	10	78	97	6530	1.77

[a] Entries 1–5 were conducted with VBBiB/dNBpy/CuBr$_2$ with Cu(0) wire (L = 2.9 mm for entry 3 and 5.8 mm for the others (d = 0.5 mm)) in anisole ([VBBiB]$_0$ = 1.8 M); entries 6 and 7 were conducted with VBBiB/dNBpy/CuCl$_2$/Cu(0) powder ([VBBiB]$_0$ = 1.8 M).
[b] M_w and Đ were determined by GPC (eluent: THF) with polystyrene calibration.

We placed the PVBBiB powders under ambient conditions to examine the self-degradation behavior. Samples over a period of time (0–9 days) were collected and diluted to the same concentration (4 mg/mL) for analysis. Figure 3a presents GPC traces of the samples of 1, 3, 5, 7, and 9 days. With respect to the signal intensities, we observed an obvious decrease in the high-MW (HMW) peaks and an increase in the low-MW (LMW) peaks over a period of days. By analyzing the normalized intensities from the HMW peaks (squares in Figure 3b), we conclude that PVBBiB decomposed significantly within 5 days; meanwhile, the byproduct was produced (circles in Figure 3b). Concerning the side reactions that we anticipated in Scheme 2, ambient conditions with O$_2$ present would be fatal for the radical reactions (i.e., trivial side reactions through processes (1) and (3)), and no branched polymer was acquired based on the results in Figures 2a (i.e., no side reaction through process (2)). To determine the mechanism of the side reaction, we used ^{1}H NMR spectroscopy to analyze the resultants. Comparing the ^{1}H NMR spectra in Figures 4a and 4b, the resultants exhibited high structural purity, allowing us to assign the structure of a five-membered ring lactone (i.e., 5-(4-(bromomethyl)phenyl)dihydro-3,3-dimethylfuran-2(3H)-one; ^{1}H NMR (400 MHz, CDCl$_3$, δ = ppm): 1.30, 1.37 (s, CH(CH$_3$)$_2$, 6H), 2.04, 2.48 (m, CH$_2$ (on lactone ring), 2H), 4.5 (s, PhCH$_2$Br, 2H), 5.44 (dd, –CH<, 1H), 7.35 (m, C$_6$H$_4$, 4H)). Since the degradation was evaluated under ambient conditions; accordingly, we propose an alternative mechanism as a side reaction, forming this lactone through PVBBiB ring-closure depolymerization.[48, 49] As displayed in Scheme 3, the pendant bromine atoms of PVBBiB acted as facile leaving atoms to form cationic polymer chains and anionic counterion intermediates (**1**). During the association/dissociation of the ions, bond breakages occurred to the OOC–CH$_2$Ph linkages, resulting in structural rearrangement to form an ionic five-membered-ring lactone intermediate (**2**). After association of the ions/counterions, a stable structure (**3**) was obtained. Thus, the polyaddition process suffered from a cyclization reaction involving backbone breakage, with competitive factors including the leaving atom affinity, catalyst activity, and reaction temperature.

2. Lactonization of model compounds through ATRA.

The model compounds BzBDT and BzCDT with different leaving atom affinity (Br, Cl) through ATRA of aromatic haloesters and MVB were synthesized and characterized (**4**, **5** in Scheme S1 and Figure S2). We examined the behavior of these model compounds to understand the degradation of the aliphatic polyesters. Based on the proposed mechanism, the five-membered-ring lactone 3,3-dimethyl-5-*p*-tolyldihydrofuran-2(3H)-one (**6** in Scheme 4) and a benzyl halide would be the major products. As revealed in Figure 5, BzBDT and BzCDT exhibit distinct stabilities. In the case of BzBDT, the obtaining crude has already featured significant amounts of the lactone and benzyl bromide (peaks 3 and 6, respectively, in Figure 5A). After

purification (Figure 5B), the lactone compound **6** was obtained in high purity. In the case of BzCDT (Figure 5C), the spectrum of the purified compound featured insignificant signals of the lactone. After seven days (Figure 5D), signals representing the formation of the lactone and benzyl chloride and of residual BzCDT were both present. When examining the BzCDT sample after an additional 24 days, we observed signals for only **6** and benzyl chloride (Figure S3, Supporting Information). Thus, the lower leaving affinity of the Cl atom, relative to the Br atom, imparted greater stability. Table 2 summarizes the reaction conditions and characterization data.
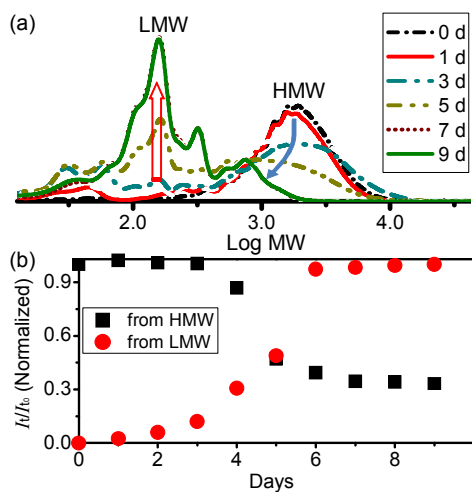

Figure 3. PVBBiB self-degradation under ambient conditions: (a) GPC traces and (b) decomposition profiles.
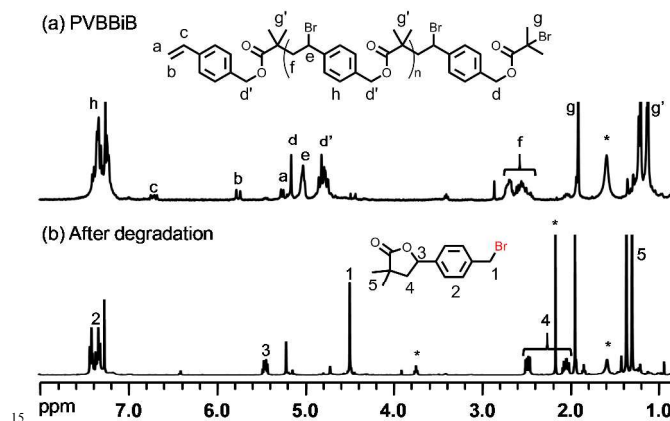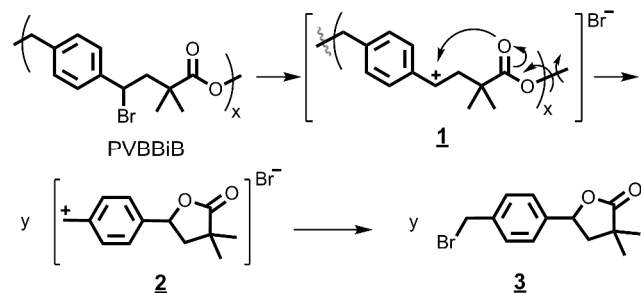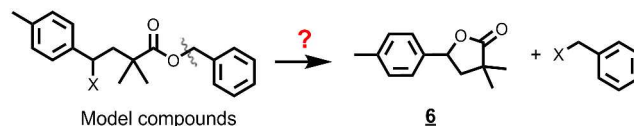

Figure 4. ^{1}H NMR spectra (400 MHz, CDCl$_3$) of (a) PVBBiB and (b) resultants (*: impurities).

Scheme 3. Proposed mechanism for five-membered-ring

lactonization from a synthesized PVBBiB polyester.

These results suggested that tuning the substituents of the aliphatic polyesters would allow us to manipulate the polymer degradation profile.

Scheme 4. Cyclizations of the model compounds BzBDT (X= Br) and BzCDT (X= Cl) illustrated in Scheme S3.
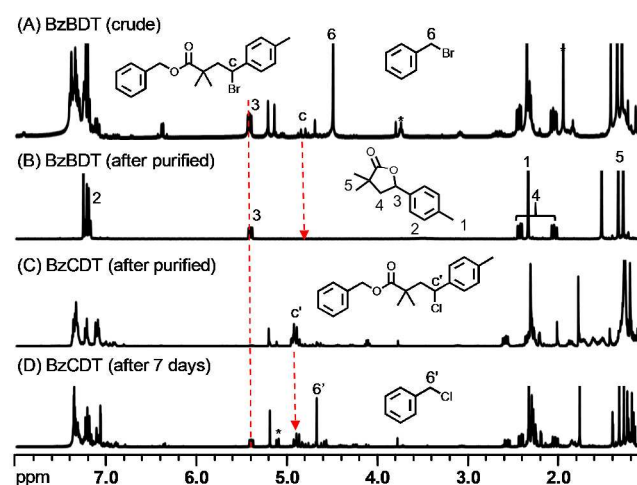

Figure 5. ^{1}H NMR spectra (400 MHz, CDCl$_3$) of the degradation products of the model compounds (A, B) BzBDT and (C, D) BzCDT.

Table 2. Synthesis of model compounds through ATRA and characterization data for their products.

Entry	Precursor /Catalyst[a]	Monoadduct[b]	Conv. (%)[c]	Apparent	
				Crude	As purified
8	BzBMP /CuBr$_2$	BzBDT	89	Yellowish liquid	Yellowish liquid
9	BzCMP /CuCl$_2$	BzCDT	75	Yellowish liquid	Light-yellowish solid

[a] Reactions were conducted using BzXMP/MVB/dNBpy/CuX$_2$/Cu(0) = 50/50/6/1/2 (X = Br or Cl) in anisole at 10 °C for a desired period of time (BzBMP: benzyl 2-bromo-2-methylpropanoate; BzCMP: benzyl 2-chloro-2-methylpropanoate; MVB: 1-methyl-4-vinylbenzene).
[b] BzBDT: 4-methylbenzyl 4-bromo-2,2-dimethyl-4-*p*-tolylbutanoate; BzCDT: 4-methylbenzyl 4-chloro-2,2-dimethyl-4-*p*-tolylbutanoate.
[c] Conversions were monitored by GC based on the consumption of the BzXMP (X = Br or Cl) precursor.

3. Tuning the substituents of the aliphatic polyesters and studying the degradation of the aliphatic polyesters.

Besides tuning the leaving atom's affinity, we also varied the backbone structure by replacing the leaving part and enhancing the steric hindrance to modify the self-degradation behavior. We

synthesized three other aliphatic polyesters (Scheme 4) that, when compared with PVBBiB, would have lesser leaving affinity (i.e., PVBCiB: $R^1 = R^2 = CH_3$, X = Cl), more stable substituents (i.e., PVBAiB: $R^1 = R^2 = CH_3$, X = N_3), and greater steric bulk (i.e., PVBBPA: $R^1 = H$, $R^2 = $ phenyl, X = Br). Details regarding the characterization of the polymer PVBAiB (Figure S4) and the inimer VBBPA (Figure S5) are available in the Supporting Information. Although we basically obtained copolymers of P(VBCiB-co-VBBiB) through halogen exchange between VBBiB and $CuCl_2/Cu(0)/dNBpy$ system, we symbolize this product as "PVBCiB" herein to simplify our discussion. We anticipated that a larger $VBBiB/CuCl_2$ ratio would lead to greater efficacy of the halogen exchange process. It has been reported that R-Br/CuCl systems have high initiating efficiency, similar to that of R-Br/CuBr systems.[50, 51] Concerning smaller propagation rate during halogen exchange[50] and surface area of Cu(0) wire, however, using Cu(0) wire would lengthen the reaction time for the case of $VBBiB/CuCl_2$; therefore, we used Cu(0) powder to accelerate the overall polymerization rate as a result of its greater surface area. Figure 6 provides kinetic comparisons of the ATRPA processes performed using different catalyst systems and ratios. Compared with $CuBr_2/Cu(0)$ wire (curve a, Figure 6A), use of $CuCl_2/Cu(0)$ powder (curve b, Figure 6A) provided a faster rate, higher conversion, and a higher-MW polymer ($M_w = 11200$; $Đ = 2.32$; curve b, Figure 6B). In the case of $VBBiB/CuCl_2$ at a 50:4 ratio, the reaction rate decreased dramatically, due to the higher amount of the $CuCl_2$ deactivator, and provided a lower-MW polymer ($M_w = 4810$; $Đ = 1.68$; curve c, Figure 6B). These results indicate that a system comprising $CuCl_2/Cu(0)$ powder/dNBpy was amenable to the ATRPA of VBBiB. We recorded ^1H NMR spectra to examine any differences in the microstructures of these products; Figures 7a–c present the ^1H NMR spectra of the corresponding PVBBiB and PVBCiB polymers in Figure 6A. The signals of these aliphatic polyesters were evident in each case. Because of overlapping of the signals for the PhCH(CH₂)Br and PhCH(CH₂)Cl units (i.e., signals e and e′ (*ca.* 5.05 ppm)), we could not discern any obvious differences in their chemical shifts. There were, however, differences in the positions of the signals of the dimethyl groups of the chain ends (i.e., signals g (*ca.* 1.93 ppm) and g′ (*ca.* 1.77 ppm)). Comparing Figures 7b and 7c, we observe that a higher amount of $CuCl_2$ led to stronger signals for protons g′. Thus, a larger $VBBiB/CuCl_2$ ratio resulted in greater halogen exchange efficacy while retaining the structure of the aliphatic polyester. Table 1 (entries 2, 6, and 7) summarizes the reaction conditions and the characterization data for these transformations.
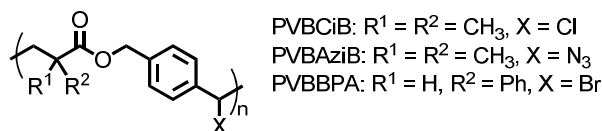
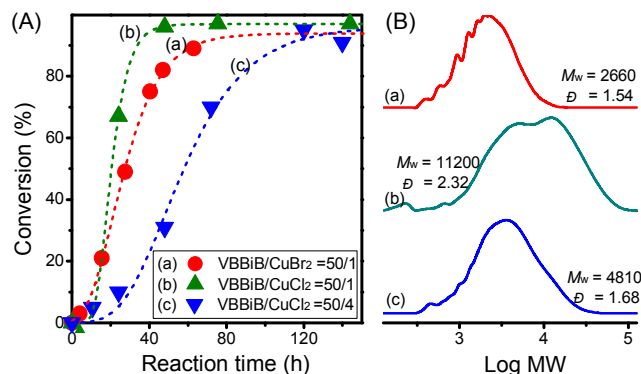Scheme 5. Tuning the substituents of the aliphatic polyesters.

PVBCiB: $R^1 = R^2 = CH_3$, X = Cl
PVBAziB: $R^1 = R^2 = CH_3$, X = N_3
PVBBPA: $R^1 = H$, $R^2 = Ph$, X = Br

Figure 6. ATRPA of $VBBiB/CuBr_2$ or $CuCl_2$ at 10 °C: (A) conversion vs time and (B) GPC traces of products ($[VBBiB]_0 = 1.8$ M; (a) $VBBiB/CuBr_2/Cu(0)$ wire (50/1/2); (b) $VBBiB/CuCl_2/Cu(0)$ powder (50/1/2); (c) $VBBiB/CuCl_2/Cu(0)$ powder (50/4/1)).
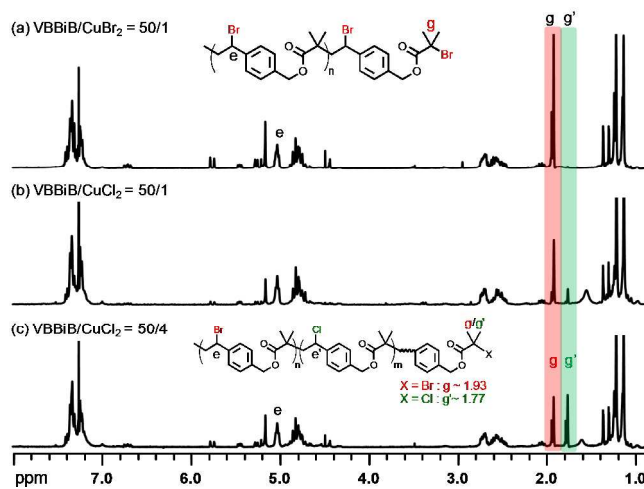

Figure 7. ^1H NMR spectra (400 MHz, CDCl₃) of the polymers PVBBiB and PVBCiB.

More important feature from the above discussion is that a stable structure can overcome the issue of low molecular weight when preparing an aliphatic polyester analogue that suffers from lactonization through backbone cleavage. Thus, we used an unsymmetrical VBBPA inimer to examine the structural limitations brought about by two factors: (i) the steric bulk near the leaving atom of the polyester backbone and (ii) the temperature. From its structure, ATRPA of VBBPA would provide two different types of initiating sites (PEBr and ethyl α-bromophenylacetate (EBPA)). Figure 8A displays the conversion data for the ATRPA of VBBPA at various temperatures (VBBPA/CuBr₂/Cu(0)/dNBpy = 50/1/2/6 in anisole; $[VBBPA]_0 = 1.8$ M). Compared with the behavior of VBBiB under similar conditions, not surprisingly the ATRPA of VBBPA occurred with faster reaction rates and had a strong temperature-dependence, which was ascribed to the very fast activation rate constant of the EBPA site ($k_{a,EBPA}/k_{a,EBiB} = $ *ca.* 2×10^3 at 35 °C).[28] At a low temperature of −10 °C (curve a), the EBPA site was also initiated and reached a conversion of approximately 90%. For the reactions performed at 40 and 90 °C (curves c and d, respectively), the conversions reached greater than 90% even within an hour. Figure 8B displays GPC traces of the

corresponding products Notably, we observed an HMW polymer (curve c: M_w = 25,550; $Đ$ = 2.90) (VBBPA/CuBr$_2$/Cu(0)/dNBpy = 50/1/2/6 in anisole at 40 °C; [VBBPA]$_0$ = 1.8 M). The results fulfilled the desire toward obtaining an HMW aliphatic polyester

5 through ATRPA of VBBPA with variations of several competitive factors, namely structural stability, catalyst affinity, and reaction temperature. Questions remained, however, about the topologies of our obtained polyadducts. Figure 9 displays the ^{1}H NMR spectra of the PVBBPA polymers. For the low-

10 temperature reactions performed at –10, 25, and 40 °C (Figures 9a–c), we obtained aliphatic polyesters PVBBPA; their detailed chemical structures are assigned in Figure 9b. We can anticipate that high-temperature reaction would either result in a product with branched signals or a byproduct of five-membered-ring

15 lactone. For the high-temperature reaction performed at 90 °C (Figure 9d), surprisingly, aliphatic polyester of PVBBPA was obtained. From the literature, we would expect an enormous difference in activation rate constants between the two initiating sites generated through ATRPA of VBBPA ($k_{a,EBPA}/k_{a,PEBr}$ = *ca.*

20 3.1 × 10^4 at 35 °C).[28] Thus, it is plausible that we can not only obtain aliphatic PVBBPA through the "frozen/polyaddition" mechanism but also suppress the initiation of the PEBr site under reactions performed at high temperature. In addition, it illustrates the intrinsically fast addition reactivity of the phenylacetate

25 radical to the vinyl bond—another important reason why we could achieve rapid and efficient ATRPA of VBBPA.
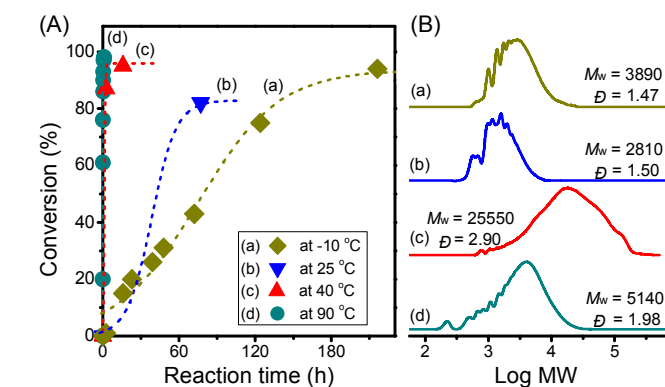

Figure 8. ATRPA of VBBPA at various temperatures: (A) conversion vs time plots and (B) GPC traces of the products

30 (VBBPA/CuBr$_2$/Cu(0) wire/dNBpy = 50/1/2/6 in anisole; [VBBPA]$_0$ = 1.8 M).

Table 3. Reaction conditions for ATRPA of VBBPA and characterization data.

Entry[a]	Compositions[a]	Temp. (°C)	Time (h)	Conv. (%)	M_w[b]	$Đ$[b]
9		-10	216	90	3890	1.47
10	50/6/1/2	25	77	82	2810	1.50
11		40	48	95	25550	2.90
12		90	1	98	5140	1.98

[a] Reactions were conducted with VBBPA/dNBpy/CuBr$_2$/Cu(0)

35 wire in anisole ([VBBPA]$_0$ = 1.8 M).
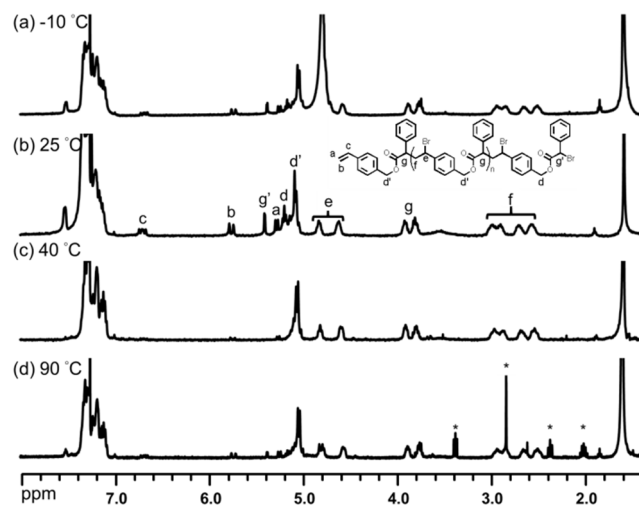[b] Values were determined by GPC (eluent: THF).

Figure 9. ^{1}H NMR spectra (400 MHz, CDCl$_3$) of PVBBPA polymers from Figure 8 (*: impurities).

40 Having obtained four kinds of aliphatic polyesters (PVBBiB, PVBCiB, PVBAiB, PVBBPA), their self-degradation behaviors were evaluated. The polymer powders were placed under ambient conditions and diluted to solutions with a constant concentration (4 mg/mL THF) before GPC measurements (Figure 10).

45 Significantly, PVBBiB and PVBCiB displayed self-degrading profiles within periods of several days (Figures 10a and 10b, respectively), but PVBBPA and PVBAiB did not (Figures 10c and 10d, respectively), possibly because of the steric bulk of the phenyl groups and the non-leaving azido groups. Figure 11

50 displays detailed degradation curves for the four aliphatic polyesters, estimated from the maximum intensities (MW > 1000) in the GPC measurements. PVBBiB exhibited a smooth self-degrading profile, whereas PVBCiB featured a step-like profile. Based on the variations in intensities, the degradation of PVBCiB

55 was more stable than that of PVBBiB (i.e., 4 days vs 1 day based on 10% degraded), due to different affinities of their leaving atoms. The presence of Cl groups stabilized the polymer backbone for a few days, with cleavage beginning from the Br-containing repeat unit first and then from the Cl-containing repeat

60 unit later. Again, PVBBPA and PVBAiB displayed stability in terms of both intensities and MWs. Figure 12 displays ^{1}H NMR spectra of the resultants from the self-degrading experiments; the results are consistent with those from the GPC analyses. The spectra of PVBBPA and PVBAiB (Figures 12c and 12d,

65 respectively) suggest the same structures as when they were initially prepared, implying stable and non-self-degrading properties. Obvious signals for five-membered-ring lactones (i.e., peaks 2–5) were present in Figures 12a and 12b for the polymers PVBBiB and PVCiB, respectively. In particular, the efficiency of

70 halogen exchange is revealed from peaks 1′ and 6′ in Figure 12b, illustrating that the chain end has higher halogen exchange efficiency than the repeat unit. Nevertheless, the small and moderate degrees of Cl atom replacement at the backbone and chain end, respectively, suppressed the self-degrading behavior.

75 Syntheses of aliphatic polyesters with full replacement of all Br atoms with Cl atoms are currently underway.
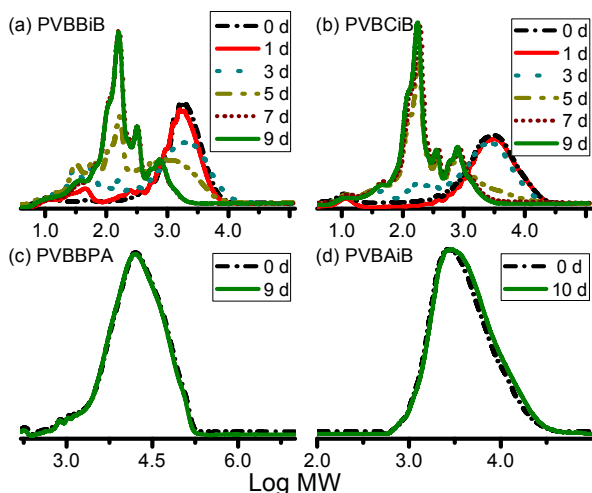
Figure 10. GPC traces recorded during self-degrading experiments of the aliphatic polyesters.
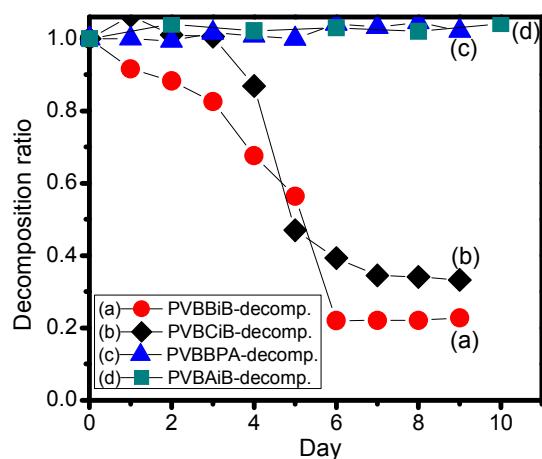

Figure 11. Degradation curves for (a) PVBBiB, (b) PVBCiB, (c) PVBAiB, and (d) PVBBPA stored under ambient conditions.
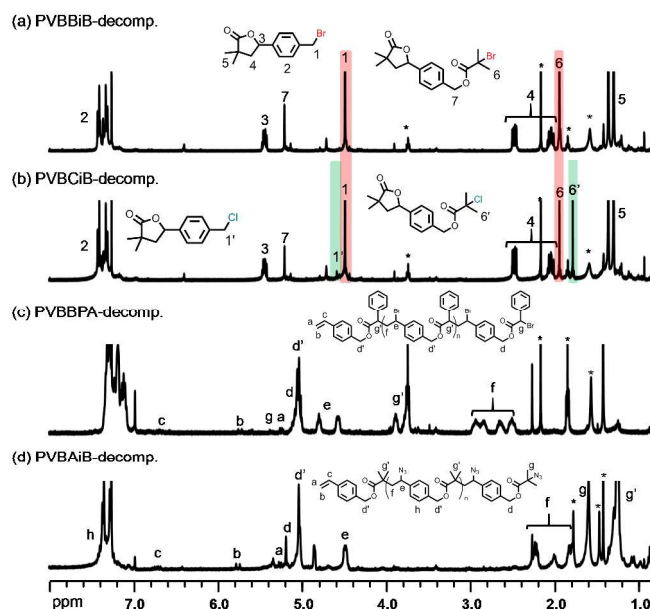

Figure 12. ^{1}H NMR spectra (400 MHz, CDCl$_3$) of the resultants from the self-degrading experiments (*: impurities).

Conclusions

We altered the scope of the ATRPA of an AB*-type vinyl bromoester (herein, the VBBiB inimer) by using a commercially available CuBr$_2$/Cu(0)/dNBpy system on shortening the reaction time (i.e., <70 h with a conversion of 90%) at moderate temperature (i.e., 10 and 25 °C). Reactions performed at low temperature resulted in structures of aliphatic polyesters obtained through a step–growth mechanism; in contrast, an unexpected structure was formed at 70 °C. By placing PVBBiB powders under ambient conditions, self-degrading behavior was evident from variations in MW in the GPC traces. The major resultants had high structural purity, with a five-membered-ring lactone (5-(4-(bromomethyl)phenyl) dihydro-3,3-dimethylfuran-2(3H)-one) identified from ^{1}H NMR spectroscopic analysis. We propose that structural rearrangement occurred through PVBBiB ring-closure depolymerization induced by the pendant leaving bromide atoms. It can be concluded that the polyaddition competed with cyclization reactions operating through backbone cleavage. By varying the leaving group's affinity, a comprehensive series of model reactions guided us to design of polymers having stable backbones. We targeted three other aliphatic polyesters possessing functionalities with a lower leaving affinity, a higher steric bulk, and a non-leaving affinity (i.e., PVBCiB, PVBBPA, and PVBAiB, respectively). For the preparations of PVBCiB and PVBBPA, we confirmed (^{1}H NMR spectra) that their structures were aliphatic polyesters, and that HMW polymers could be obtained ($M_{w,PVBCiB}$ = 11,200, Đ = 2.32; $M_{w,PVBBPA}$ = 25,550, Đ = 2.90). Thus, we had fulfilled the challenge of obtaining HMW aliphatic polyesters through ATRPA by varying several the competitive factors: structural stability, catalyst affinity, and reaction temperature. Of the four aliphatic polyesters, PVBBiB and PVBCiB displayed obvious self-degrading profiles within periods of several days, but PVBBPA and PVBAiB did not. Through this study, we unveiled the limitations resulting from lactonization on the ATRPA process with AB*-type inimers. Thus, proper usages of commercially available copper catalysts and the unique self-depolymerization behavior provide inexpensive and straightforward routes to the design of self-degradable aliphatic polyesters with multi-functionalities.

Notes and references

[a] Department of Chemical Engineering, National Chung Hsing University, 250 Kuo Kuang Road, Taichung 40227, Taiwan. Tel: +886-4-22854936; E-mail: HuangCF@dragon.nchu.edu.tw

† Electronic Supplementary Information (ESI) available: Synthesis and characterization of model compounds. ^{1}H NMR and FT-IR spectra of VBBiB, VBBPA, and PVBAiB.

1. A. C. Albertsson and I. K. Varma, *Adv Polym Sci*, 2002, **157**, 1-40.
2. C. Jerome and P. Lecomte, *Adv Drug Deliver Rev*, 2008, **60**, 1056-1076.

3.   K. E. Uhrich, S. M. Cannizzaro, R. S. Langer and K. M. Shakesheff, *Chem Rev*, 1999, **99**, 3181-3198.

4.   C. M. Thomas, *Chem Soc Rev*, 2010, **39**, 165-173.

5.   C. K. Williams, *Chem Soc Rev*, 2007, **36**, 1573-1580.

6.   J. Chen, S. W. Huang, M. Liu and R. X. Zhuo, *Polymer*, 2007, **48**, 675-681.

7.   D. M. Lynn and R. Langer, *J Am Chem Soc*, 2000, **122**, 10761-10768.

8.   B. D. Mather, K. Viswanathan, K. M. Miller and T. E. Long, *Prog Polym Sci*, 2006, **31**, 487-531.

9.   F. H. Meng, W. E. Hennink and Z. Zhong, *Biomaterials*, 2009, **30**, 2180-2198.

10.   A. M. DiCiccio and G. W. Coates, *J Am Chem Soc*, 2011, **133**, 10724-10727.

11.   S. Huijser, E. HosseiniNejad, R. Sablong, C. de Jong, C. E. Koning and R. Duchateau, *Macromolecules*, 2011, **44**, 1132-1139.

12.   R. C. Jeske, A. M. DiCiccio and G. W. Coates, *J Am Chem Soc*, 2007, **129**, 11330-11331.

13.   X. X. Deng, L. Li, Z. L. Li, A. Lv, F. S. Du and Z. C. Li, *ACS Macro Letters*, 2012, **1**, 1300-1303.

14.   O. Kreye, T. Toth and M. A. R. Meier, *J Am Chem Soc*, 2011, **133**, 1790-1792.

15.   S. C. Solleder and M. A. R. Meier, *Angew Chem Int Edit*, 2014, **53**, 711-714.

16.   S. H. Ji, B. Bruchmann and H. A. Klok, *Macromol Chem Phys*, 2011, **212**, 2612-2618.

17.   S. H. Ji, B. Bruchmann and H. A. Klok, *Macromolecules*, 2011, **44**, 5218-5226.

18.   J. F. Lutz, J. Andrieu, S. Uzgun, C. Rudolph and S. Agarwal, *Macromolecules*, 2007, **40**, 8540-8543.

19.   J. Y. Yuan, C. Y. Pan and B. Z. Tang, *Macromolecules*, 2001, **34**, 211-214.

20.   H. Wickel and S. Agarwal, *Macromolecules*, 2003, **36**, 6152-6159.

21.   Q. Smith, J. Y. Huang, K. Matyjaszewski and Y. L. Loo, *Macromolecules*, 2005, **38**, 5581-5586.

22.   J. M. J. Paulusse, R. J. Amir, R. A. Evans and C. J. Hawker, *J Am Chem Soc*, 2009, **131**, 9805-9812.

23.   M. Kamigaito, T. Ando and M. Sawamoto, *Chem Rev*, 2001, **101**, 3689-3745.

24.   J.-S. Wang and K. Matyjaszewski, *Macromolecules*, 1995, **28**, 7901-7910.

25.   J.-S. Wang and K. Matyjaszewski, *J Am Chem Soc*, 1995, **117**, 5614-5615.

26.   N. V. Tsarevsky and K. Matyjaszewski, *Chem Rev*, 2007, **107**, 2270-2299.

27.   F. Minisci, *Acc Chem Res*, 1975, **8**, 165-171.

28.   W. Tang, Y. Kwak, W. Braunecker, N. V. Tsarevsky, M. L. Coote and K. Matyjaszewski, *J Am Chem Soc*, 2008, **130**, 10702-10713.

29.   K. Matyjaszewski, *Macromolecules*, 2012, **45**, 4015-4039.

30.   W. T. Eckenhoff, A. B. Biernesser and T. Pintauer, *Abstr Pap Am Chem S*, 2010, **239**.

31.   V. Percec, T. Guliashvili, J. S. Ladislaw, A. Wistrand, A. Stjerndahl, M. J. Sienkowska, M. J. Monteiro and S. Sahoo, *J Am Chem Soc*, 2006, **128**, 14156-14165.

32.   K. Matyjaszewski, S. Coca, S. G. Gaynor, M. L. Wei and B. E. Woodworth, *Macromolecules*, 1997, **30**, 7348-7350.

33.   P. M. Wright, G. Mantovani and D. M. Haddleton, *J Polym Sci Pol Chem*, 2008, **46**, 7376-7385.

34.   C. Yoshikawa, A. Goto and T. Fukuda, *e-Polymers*, 2002, no. 13.

35.   W. C. Lin, Q. Fu, Y. Zhang and J. L. Huang, *Macromolecules*, 2008, **41**, 4127-4135.

36.   Z.-C. Chen, C.-L. Chiu and C.-F. Huang, *Polymers*, 2014, **6**, 2552-2572.

37.   B.-T. Dong, Y.-Q. Dong, F.-S. Du and Z.-C. Li, *Macromolecules*, 2010, **43**, 8790-8798.

38.   K. Matyjaszewski, S. G. Gaynor, A. Kulfan and M. Podwika, *Macromolecules*, 1997, **30**, 5192-5194.

39.   K. Satoh, M. Mizutani and M. Kamigaito, *Chem Commun*, 2007, 1260-1262.

40.   B. T. Dong, Z. L. Li, L. J. Zhang, F. S. Du and Z. C. Li, *Polym Chem*, 2012, **3**, 2523-2530.

41.   M. Mizutani, K. Satoh and M. Kamigaito, *J Am Chem Soc*, 2010, **132**, 7498-7507.

42.   X. M. Zhang, H. Q. Dou, Z. B. Zhang, W. Zhang, X. L. Zhu and J. Zhu, *J Polym Sci Pol Chem*, 2013, **51**, 3907-3916.

43.   M. Mizutani, E. F. Palermo, L. M. Thoma, K. Satoh, M. Kamigaito and K. Kuroda, *Biomacromolecules*, 2012, **13**, 1554-1563.

44.   L. J. Zhang, B. T. Dong, F. S. Du and Z. C. Li, *Macromolecules*, 2012, **45**, 8580-8587.

45.   K. Satoh, S. Ozawa, M. Mizutani, K. Nagai and M. Kamigaito, *Nat Commun*, 2010, **1**, 1-6.

46.   J. O. Park and S. H. Jang, *J Polym Sci Pol Chem*, 1992, **30**, 723-729.

47.   C. F. Huang, R. Nicolay, Y. Kwak, F. C. Chang and K. Matyjaszewski, *Macromolecules*, 2009, **42**, 8198-8210.

48.   C. Galli, Illumina.G and Mandolin.L, *J Am Chem Soc*, 1973, **95**, 8374-8379.

49.   C. Galli, G. Illuminati, L. Mandolini and P. Tamborra, *J Am Chem Soc*, 1977, **99**, 2591-2597.

50.   K. Matyjaszewski, D. A. Shipp, J. L. Wang, T. Grimaud and T. E. Patten, *Macromolecules*, 1998, **31**, 6836-6840.

51.   K. Matyjaszewski, J. L. Wang, T. Grimaud and D. A. Shipp, *Macromolecules*, 1998, **31**, 1527-1534.

for Table of Contents use only

Polymerization and Degradation of Aliphatic Polyesters Synthesized by Atom Transfer Radical Polyaddition

Yu-Min Han, Hsin-Hua Chen, and Chih-Feng Huang*

By tuning leaving group affinity, the aliphatic polyesters synthesized by ATRPA can avoid the lactonization and obtain high moleular weight.